REGRIDDING OF REMOTE SENSING RETRIEVALS: FORMALISM AND APPLICATION TO GOME VS MICROWAVE OZONE PROFILE COMPARISON

Yasmine Calisesi(1), **Roeland van Oss**(2), **and Vincent T. Soebijanta**(3)

(1) *International Space Science Institute, Hallerstrasse 6, CH - 3012 Bern, Switzerland*
(2) *Royal Netherlands Meteorological Institute, Postbus 201, NL-3730 AE De Bilt, Netherlands*
(3) *Belgian Institute for Space Aeronomy, Ringlaan 3, B-1180 Brussels, Belgium*

Abstract. One of the difficulties commonly arising in geophysical intercomparison studies is the inhomogeneity of the comparison data. As a matter of fact, two independent measurements of an atmospheric constituent profile to be compared to each other will generally be expressed in different units, and onto fully different vertical grids. For many applications, these differences can be most simply eliminated by the application of interpolation or averaging operators, or of auxiliary profiles such as temperature and pressure to achieve homogenized profile units. In the case of profiles retrieved from remote sounding measurements using advanced techniques such as optimal estimation, however, the situaton is complicated by the different dependency on a-priori information, expressed in differing averaging kernels. In order to solve this problem, a formalism was developed that allows the homogenization of retrieval products (and in particular of their numerical grids) without preliminary alteration of the respective retrieval algorithms. In a recent study [1], this formalism was applied to the comparison of independent ozone profile measurements by the Global Ozone Monitoring Experiment (GOME) and a ground-based microwave radiometer (MW) during 2000. We present the results of this study, and describe the employed linear profile transformation method.

1 INTRODUCTION

There are two main difficulties associated with the intercomparison of remote soundings. The first difficulty is related to the essence of this data: these being indeed the result of a trade-off between information extracted from the performed measurements, and some additional ("a-priori") information used to constrain the retrieval results towards physically acceptable solutions. In the case of atmospheric profilers, the share of useful information actually contributed by the measurements, or the influence of other determining factors such as vertical resolution or retrieval errors, vary with altitude and depend on the observing system configuration. In intercomparison procedures, these characteristics must be taken into account in order to ensure a correct interpretation of the comparison results.

The second difficulty applies more generally to any intercomparison process, and resides in the inhomogeneity of the comparison data. As a matter of fact, two independent measurements of an atmospheric profile subject to intercomparison will generally be mapped onto fully different vertical grids, with different time resolutions, and using different units. In the case of remote sounders, the homogenization of independently retrieved state vectors is complicated by the different dependency on a-priori information, expressed in differing averaging kernels. Accurate intercomparisons of remote sounders thus require in the homogenization of auxiliary retrieval products, such as averaging kernels or covariance matrixes, for which an adequate formalism has to be developed. Although seemingly trivial, the problem of the homogenization of remote sounding measurements thus still deserves consideration in order to achieve reliable comparison results.

Recently, [2] allowed to account for differing observation systems characteristics by eliminating identified bias contributions from the obtained comparison results. This approach is essential to a better interpretation of remote sounders intercomparisons results. However, it was in a first time restricted to intercomparisons of identical state vectors. [1] proposed to relax this condition, by the use of linear transformation functions to homogenize the products of independent retrievals.

2 REGRIDDING OF RETRIEVAL PRODUCTS

2.1 Retrieval Formalism

According to [3], we note $\mathbf{y}$ the $m \times 1$ vector of the measured signal ("measurement vector"), and $\mathbf{x}$ the $n \times 1$ vector of atmospheric state to be retrieved ("state vector"). The relationship between the measured signal $\mathbf{y}$ and the searched atmospheric profile $\mathbf{x}$ is provided by the forward model $\mathbf{F}(\mathbf{x})$, which describes the physics of the measurement and accounts for all known processes influencing the observed signal from its emission to its detection in the instrument. The forward model reproduces the actual measurements within accuracy $\boldsymbol{\epsilon}_\mathbf{y}$, which encapsulates both systematic and random components of the measurement and forward model errors:

$$\mathbf{y} = \mathbf{F}(\mathbf{x}) + \boldsymbol{\epsilon}_\mathbf{y} \tag{1}$$

Linearization of the forward model about some reference profile $\mathbf{x_0}$, and minimization of a cost function under the constraint of a-priori information, leads to the inverse model solution [4]

$$\hat{\mathbf{x}} = \mathbf{x_a} + \mathbf{A_x}(\mathbf{x} - \mathbf{x_a}) + \mathbf{G_x}\boldsymbol{\epsilon}_\mathbf{y} \tag{2}$$

where $\hat{\mathbf{x}}$ is the retrieved state vector, $\mathbf{x_a}$ is the considered a priori profile, $\mathbf{A_x} = \mathbf{G_x}\mathbf{K_x}$ is the $n \times n$ matrix of the averaging kernels, $\mathbf{G_x}$ is the $n \times m$ retrieval gain matrix, and $\mathbf{K_x}$ is the $m \times n$ Jacobian matrix of the forward model evaluated at $\mathbf{x_0}$.

2.2 State Vector Transformation

Suppose now that two independent observations of the same atmospheric profile are performed. We name $\mathbf{z_1}$ and $\mathbf{z_2}$ the corresponding independent representations of the state vector, of length l_1 and l_2, respectively. As shown by [5], any $\mathbf{z_1}$ and $\mathbf{z_2}$ can be related to each other by the $l_1 \times l_2$ transformation $\mathbf{W_{12}}$, such as

$$\mathbf{z_1} = \mathbf{W_{12}}\mathbf{z_2} + \boldsymbol{\epsilon}_{\mathbf{W_{12}}}\mathbf{x} \tag{3}$$

with $\mathbf{W_{12}} = \mathbf{W_1^*}\mathbf{W_2}$ and $\boldsymbol{\epsilon}_{\mathbf{W_{12}}} = \mathbf{W_1^*}(\mathbf{I} - \mathbf{W_2}\mathbf{W_2^*})$, and, inversely,

$$\mathbf{z_2} = \mathbf{W_{21}}\mathbf{z_1} + \boldsymbol{\epsilon}_{\mathbf{W_{21}}}\mathbf{x} \tag{4}$$

with $\mathbf{W_{21}} = \mathbf{W_2^*}\mathbf{W_1}$ and $\boldsymbol{\epsilon}_{\mathbf{W_{21}}} = \mathbf{W_2^*}(\mathbf{I} - \mathbf{W_1}\mathbf{W_1^*})$, where $\mathbf{W_1}$ and $\mathbf{W_2}$ are linear interpolation matrixes allowing to transform $\mathbf{z_1}$ and $\mathbf{z_2}$ to a common superset numerical grid [1], and where $\mathbf{W_1^*}$ and $\mathbf{W_2^*}$ are their respective generalized pseudo inverses.

2.3 Regridding of Retrieval Products

Using (3) and (4) and considering equivalent relationships to (2) transcribed to the state spaces of $\mathbf{z_2}$ and $\mathbf{z_2}$, we derive the following relationships for the transformation of retrieval products across independent numerical grids [1]:

$$\begin{aligned}
\hat{\mathbf{z}}_\mathbf{1} &= \mathbf{W_{12}}\hat{\mathbf{z}}_\mathbf{2} + \boldsymbol{\epsilon}_{\mathbf{W_{12}}}\hat{\mathbf{x}} && (5)\\
\mathbf{K}_{\mathbf{z_1}} &= \mathbf{K}_{\mathbf{z_2}}\mathbf{W_{21}} + \mathbf{K_x}\boldsymbol{\epsilon}^*_{\mathbf{W_{12}}} && (6)\\
\mathbf{G}_{\mathbf{z_1}} &= \mathbf{W_{12}}\mathbf{G}_{\mathbf{z_2}} + \boldsymbol{\epsilon}_{\mathbf{W_{12}}}\mathbf{G_x} && (7)\\
\mathbf{A}_{\mathbf{z_1}} &= \mathbf{W_{12}}\mathbf{A}_{\mathbf{z_2}}\mathbf{W_{21}} + \mathbf{W_1^*}\boldsymbol{\epsilon}_{\mathbf{A_2}}\mathbf{W_1} && (8)
\end{aligned}$$

where $\boldsymbol{\epsilon}^*_{\mathbf{W_{12}}} = (\mathbf{I} - \mathbf{W_2}\mathbf{W_2^*})\mathbf{W_1}$ and $\boldsymbol{\epsilon}_{\mathbf{W_{12}}} = \mathbf{W_1^*}(\mathbf{I} - \mathbf{W_2}\mathbf{W_2^*})$ as in (3).
Consistently, the difference $\boldsymbol{\delta}$ between $\hat{\mathbf{z}}_\mathbf{1}$ and $\hat{\mathbf{z}}'_\mathbf{1}$, where $\hat{\mathbf{z}}'_\mathbf{1}$ is the independent retrieval $\hat{\mathbf{z}}_\mathbf{2}$ transposed to the state space of $\hat{\mathbf{z}}_\mathbf{1}$ using $\hat{\mathbf{z}}'_\mathbf{1} = \mathbf{W_{12}}\hat{\mathbf{z}}_\mathbf{2}$, has for covariance

$$\begin{aligned}
\mathbf{S}_{\boldsymbol{\delta}} = \;& (\mathbf{A}_{\mathbf{z_1}} - \mathbf{I_1})\mathbf{S}_{\mathbf{a_1}}(\mathbf{A}_{\mathbf{z_1}} - \mathbf{I_1})^T \\
&+ \mathbf{W_{12}}(\mathbf{A}_{\mathbf{z_2}} - \mathbf{I_2})\mathbf{S}_{\mathbf{a_2}}(\mathbf{A}_{\mathbf{z_2}} - \mathbf{I_2})^T\mathbf{W_{12}^T} \\
&+ \mathbf{S}_{\mathbf{z_1}} + \mathbf{W_{12}}\mathbf{S}_{\mathbf{z_2}}\mathbf{W_{12}^T}
\end{aligned} \tag{9}$$

where $\mathbf{S}_{\mathbf{a_1}}$ and $\mathbf{S}_{\mathbf{a_2}}$ are the a priori covariance matrixes of retrievals 1 and 2, respectively, $\mathbf{S}_{\mathbf{z_1}} = \mathbf{G}_{\mathbf{z_1}}\mathbf{S}_{\mathbf{y_1}}\mathbf{G}_{\mathbf{z_1}}^T$ and $\mathbf{S}_{\mathbf{z_2}} = \mathbf{G}_{\mathbf{z_2}}\mathbf{S}_{\mathbf{y_2}}\mathbf{G}_{\mathbf{z_2}}^T$ are the systems respective measurements error covariances, and $\mathbf{I_1}$ and $\mathbf{I_2}$ are the identity matrixes in the corresponding state spaces.

3 APPLICATION: INTERCOMPARISON OF GROUND- AND SATELLITE-BASED OZONE PROFILE OBSERVATIONS

We used the above formalism combined with the method proposed by [2] to compare independent ozone profile observations performed during 2000 with the satellite-borne Global Ozone Monitoring Experiment (GOME) [6] and the ground-based millimeter-wave Stratospheric Ozone Monitoring Radiometer (SOMORA) [7]. Both instruments provide measurements of the stratospheric ozone profile, though on different vertical grids and in different units.

3.1 Instruments Characteristics

SOMORA provides quasi-continuous observations of the stratospheric and mesospheric ozone volume mixing ratio (VMR) profile. The instrument monitors the rotational transition line of ozone at 142.175 GHz. Information about the species vertical distribution is extracted from the recorded pressure-broadened emission spectra using an iterative optimal estimation retrieval algorithm [4, 8]. The retrieved state vector consists of 29 ozone profile components, complemented with 4 auxiliary observational parameters. The ozone VMR values are retrieved within fixed altitude layers of 2-20 km thickness spanning the range between the ground and 110 km altitude. The a-priori profile and covariance information was computed from a series of 5-year independent microwave measurements, extended to the lower stratosphere and the troposphere using coincident Brewer-Mast ozonesonde measurements [9]. After 30 minutes integration time, sufficient signal-to-noise ratio is achieved in the SOMORA spectral line measurements to retrieve ozone profiles with low a-priori information content between 20 and 65 km altitude. The corresponding vertical resolution, taken as the full-width at half-maximum of the averaging kernels (Figure 1a), is of the order of 10 km in this altitude range. The SOMORA instrument was first put into operation at the Institute of Applied Physics of the University of Bern (46.95°N 7.45°E) in August 1999, and is operated on a continuous basis since January 2000.
GOME measures the solar irradiance and backscattered earthshine radiance spectra in the 240–790 nm spectral band in a nadir viewing geometry. Information about the vertical distribution of ozone in the stratosphere is retrieved from the 265–330 nm ozone absorption band. GOME level-2 ozone data used in the present study were processed at the Royal Netherlands Meteorological Institute (KNMI) using the Ozone ProfilE Retrieval Algorithm (OPERA). Like the SOMORA retrieval, this algorithm is based on an iterative optimal estimation scheme [4]. OPERA retrieves the profile of partial ozone column amounts within 40 layers of 1–2 km width, ranging from the ground to 0.1 hPa ($\sim$ 65 km). The layer boundaries are fixed in pressure, with exception of the surface and cloud top pressure levels which are adjusted to actual conditions. A-priori information is provided by an hybrid ozonesonde and satellite measurements climatology [10]. The a-priori error covariance is obtained from an older version of the climatology. A fixed correlation matrix is used for the off-diagonal elements. With an integration time of 12 seconds, corresponding to a nadir spatial resolution of approximately 100x960 square kilometers, sufficient information is contained in the GOME measurements to retrieve ozone profiles with low a-priori information content from about 15 km up to 50 km altitude. The vertical resolution of the GOME retrieval results lies between 4 and 8 km depending on altitude. The GOME averaging kernels are represented in Figure 1b. GOME was launched on-board the second European Remote Sensing satellite (ERS-2) onto a sun-synchronous, near polar orbit on April 21, 1995.

3.2 Data Selection

The accepted coincidence and collocation criteria between the SOMORA and GOME ozone profile measurements were set to $\pm$ 15 minutes acquisition time and $\pm$ 400 km ground pixel offset, respectively. These selection criteria yielded a set of 83 coincident and collocated SOMORA and GOME measurements acquired between January 1 and December 31, 2000.

3.3 Intercomparison Procedure

In order to allow a quantitative comparison of the respective retrieval results, a transformation of the GOME ozone profiles to the SOMORA coordinates, or conversely, was required. We used for this purpose the formalism presented in Section 2, under the assumption that the transformation errors could be neglected.
A sketch of the applied transformations is provided in Figure 3. We used relationships (5) to (8) and their reverse equivalents with the identities $\mathbf{W_1} = \mathbf{W_S}$ and $\mathbf{W_2} = \mathbf{W_G}$. $\mathbf{W_S}$ and $\mathbf{W_G}$ were both defined as 4-point polynomial interpolation matrixes, and their pseudo-inverses were defined as the generalized inverses $\mathbf{W_G^*} = (\mathbf{W_G}^T\mathbf{W_G})^{-1}\mathbf{W_G}^T$ and $\mathbf{W_S^*} = (\mathbf{W_S}^T\mathbf{W_S})^{-1}\mathbf{W_S}^T$. $\mathbf{U}$ was constructed as the diagonal matrix that converts profiles of partial ozone columns into

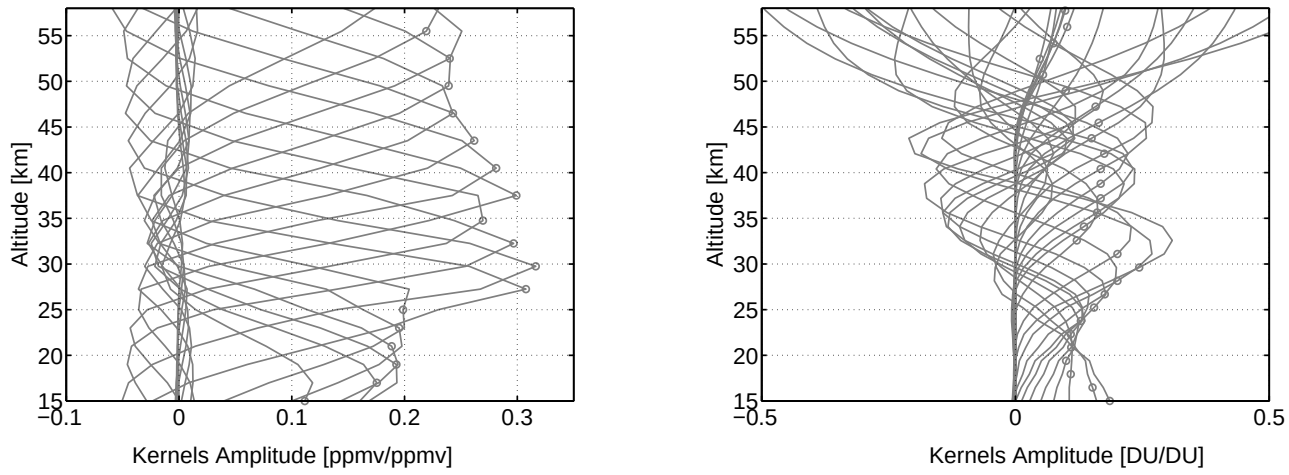

a) **b)**

Figure 1: **a)** Averaging kernels for the SOMORA ozone VMR retrievals. The nominal height of each kernel is marked by a circle. **b)** Averaging kernels for the GOME ozone profile retrievals. The kernels do not peak at their nominal altitude due to the absolute units of the retrieved profiles.

profiles of layer-equivalent VMR values. Due to the day-to-day variability of the GOME retrieval grid, the superset vector grid was redefined anew for each comparison day.
After transformation, a comparison of the obtained profiles was performed within each of the GOME and the SOMORA state spaces according to the procedure proposed by [2]. The homogenized profiles were thus successively corrected for the use of different a-priori information, adjusted for non-iterative linear retrieval, and the GOME results were convoluted with the lower-resolution SOMORA averaging kernels using equations (10), (18), and (28) of [2]. The comparison ensemble was defined as the SOMORA a priori ensemble. The variance of the presented comparison results was compared to estimates derived from (9), or from the adjusted version of equation (30) in [2]:

$$\begin{aligned}\mathbf{S}_{\delta_{12}} &= \mathbf{S}_{\mathbf{z_1}} + \mathbf{A}_{\mathbf{z_1}}\mathbf{W_{12}}\mathbf{S}_{\mathbf{z_2}}\mathbf{W}_{\mathbf{12}}^{T}\mathbf{A}_{\mathbf{z_1}}^{T} \\ &+ (\mathbf{I_1} - \mathbf{W_{12}}\mathbf{A}_{\mathbf{z_2}}\mathbf{W_{21}})\mathbf{A}_{\mathbf{z_1}}\mathbf{S_c}\mathbf{A}_{\mathbf{z_1}}^{T}(\mathbf{I_1} - \mathbf{W_{12}}\mathbf{A}_{\mathbf{z_2}}\mathbf{W_{21}})^{T}\end{aligned} \tag{10}$$

An example of a simulation of the SOMORA averaging kernels using the GOME instrument is shown in Figure 4.

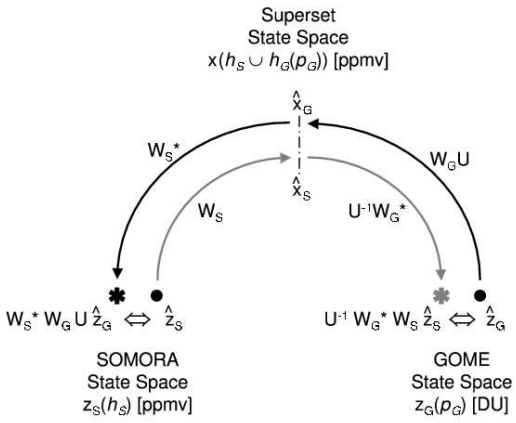

Figure 3: Summary of the undertaken state vector transformations. The homogenization allows intercomparison within each of the original retrievals state spaces.

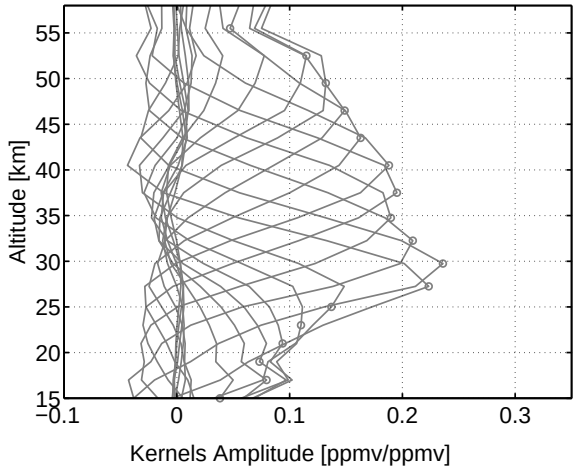

Figure 4: GOME averaging kernels as seen through the SOMORA instrument. The GOME kernels were transposed to the SOMORA state space, adjusted to the comparison ensemble, and convolved with the SOMORA averaging kernels following [2]. Reproduced from [1].

4 RESULTS

4.1 SOMORA State Space

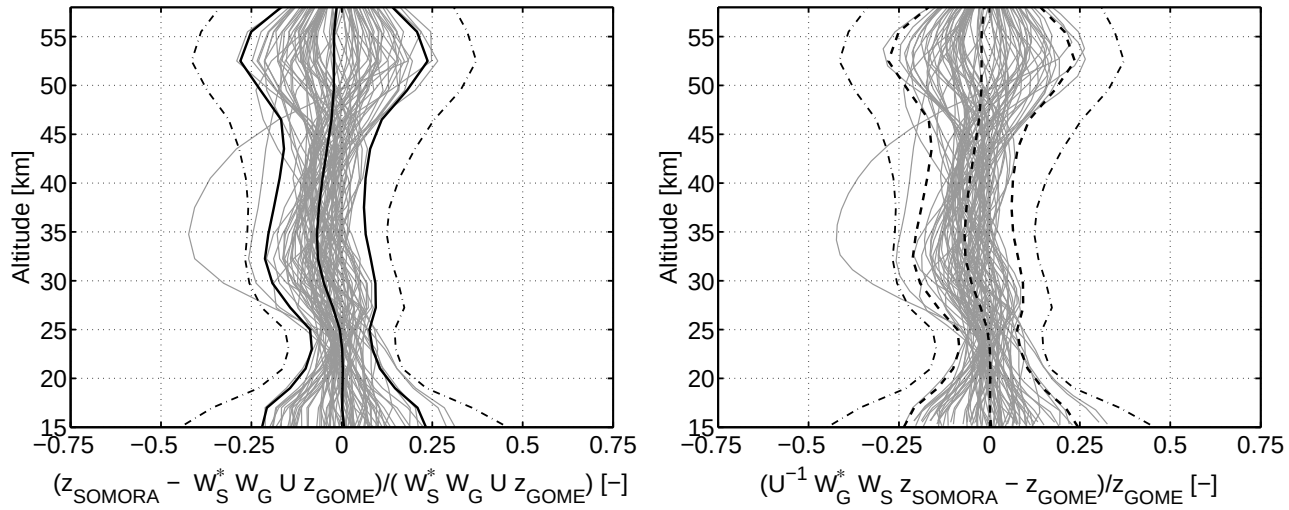

a) **b)**

Figure 5: a) Relative difference between coincident SOMORA and GOME ozone profiles after application of the procedure proposed by [2], GOME profiles converted to the SOMORA state space. **b)** As a), but with SOMORA profiles converted to the GOME state space. Shown are the individiual comparison pairs results (light gray), the samples average and $\pm 2\sigma$ width (black solid curves), and the expected results variance ($\pm 2\sigma$) according to (9) (dash-dotted curves). Reproduced from [1].

Figure 5a shows the results of the comparison between coincident SOMORA and GOME ozone profiles within the SOMORA state space, after application of the [2] procedure. Note that the results presented in this Figure require the transformation of the GOME retrieval gain and averaging kernels matrixes to the SOMORA retrieval coordinates. In the present case, a direct statistical analysis of the obtained comparison results is allowed by the time invariance of the homogenized retrievals altitude grid (SOMORA retrieval grid). The width of the obtained results distribution ($\pm 2\sigma$, outermost solid black curves in Figure 5a can thus be compared to the expected results variance ($\pm 2\sigma$, dash-dotted), estimated according to (10). For qualitative comparison with the following Sections results, the relative difference between each coincident GOME and SOMORA measurement pairs is also represented in this Figure (grey curves).

4.2 GOME State Space

In line with the proposed method validation procedure, we expect the intercomparison results to be largely independent of the choice of the comparison state space. A verification of this hypothesis is achieved by comparing the previous Section results with those obtained within the GOME state space, i.e. after converting the SOMORA results to the GOME retrieval units and vertical grid (Figure 5b). In the present case, no altitude-bound statistical analysis of the obtained comparison results can be performed directly, due to the day-to-day variability of the GOME retrievals altitude grid. Visual inspection of the grey curves displayed in the two panels of Figure 5, respectively, reveals nevertheless a good qualitative agreement between the different state spaces results. An insight into their quantitative agreement can be gained by considering interpolated versions of the individual bias profiles shown in Figure 5b. The obtained distribution average and width (dashed curves) reproduce almost identically those achieved in the SOMORA state space, which indicates that no significant artefact was introduced in the intercomparison results by the employed homogenization technique.

5 CONCLUSIONS

We proposed in [1] a simple method to regrid remote sensing observations of atmospheric constituents profiles. The method allows the homogenization of independently retrieved state vectors and of other associated retrieval products,

without the need for altering either retrieval algorithm. By providing a complete control of the undertaken transformation process, the proposed technique improves the reliability of inhomogenous state vectors intercomparison results.
The proposed technique was applied to the comparison of independent remote sensing observations of the stratospheric ozone profile, performed during 2000 with the satellite borne Global Ozone Monitoring Experiment (GOME) and the MeteoSwiss ground-based Stratospheric Ozone Monitoring Radiometer (SOMORA). After removal of smoothing error contributions, an overall $\pm 7\%$ average agreement was achieved in the altitude range 20 to 50 km between the 83 coincident SOMORA and GOME measurements pairs taken into account in the comparison. A validation of the proposed homogenization method was achieved by comparing a second set of microwave data set, evaluated directly on the GOME retrieval grid, with the original GOME profiles, and by showing that no systematic differences were observed with respect to the intercomparison results obtained in each original measurements state space.

Acknowledgments. The authors would like to thank C.D. Rodgers, S. Migliorini, A. Parrish, and K. Arzner for their very useful comments on the manuscript and for fruitful discussions about the proposed regridding technique. Many thanks also to N. Kämpfer and M. de Mazière. This work was funded by PRODEX, MeteoSwiss, and the Swiss National Science Foundation under grant 200020-100153.

References

[1] Calisesi, Y., V. T. Soebijanta, and R. van Oss, Regridding of remote soundings: Formulation and application to ozone profile comparison, . *J. Geophys. Res.*, 110, doi:10.1029/2005JD006122, 2005.

[2] Rodgers, C. D., and B. J. Connor, Intercomparison of remote sounding instruments, *J. Geophys. Res.*, *108*(D3), 4116, 2003, doi:10.1029/2002JD002299.

[3] Rodgers, C. D., *Inverse methods for atmospheric sounding*, vol. 2 of *Series on atmospheric, oceanic, and planetary physics*, World Scientific, Singapore, 2000.

[4] Rodgers, C. D., Retrieval of atmospheric temperature and composition from remote measurements of thermal radiation, *Rev. Geophys. Space Phys.*, *14*(4), 609–624, 1976.

[5] Migliorini, S., C. Piccolo, and C. D. Rodgers, Quasi-optimal assimilation of remote sounders: Formulation, submitted to *Q. J. R. Meteorol. Soc.*, 2005.

[6] Burrows, J. P., et al., The Global Ozone Monitoring Experiment (GOME): mission concept and first scientific results, *J. Atmos. Sci.*, *56*, 151–175, 1999.

[7] Calisesi, Y., The Stratospheric Ozone Monitoring Radiometer SOMORA: NDSC application document, Research Report 2003-11, Institute of Applied Physics, University of Bern, Switzerland, 2003.

[8] Calisesi, Y., The Stratospheric Ozone MOnitoring RAdiometer SOMORA: Data retrieval, Research Report 2000-3, Institute of Applied Physics, University of Bern, Switzerland, 2000.

[9] Calisesi, Y., R. Stübi, N. Kämpfer, and P. Viatte, Investigation of systematic uncertainties in Brewer-Mast ozone soundings using observations from a ground-based microwave radiometer, *J. Atmos. Ocean. Technol.*, 2003.

[10] Fortuin, J. P. F., and H. Kelder, An ozone climatology based on ozonesonde and satellite measurements, *J. Geophys. Res.*, *103*, 31709–31734, 1998.